Electron Transfer Properties of the R2 Protein of Ribonucleotide Reductase from *Escherichia coli*†

Kathleen E. Silva, Timothy E. Elgren,‡ Lawrence Que, Jr., and Marian T. Stankovich*

Department of Chemistry, University of Minnesota, Minneapolis, Minnesota 55455

Received May 8, 1995; Revised Manuscript Received August 21, 1995®

ABSTRACT: The enzyme ribonucleotide reductase from *Escherichia coli* consists of two proteins, R1 and R2. The active R2 protein contains two dinuclear iron centers and the catalytically essential tyrosyl radical. We have explored the redox properties of the tyrosyl radical and estimate an apparent redox potential of +1000 ±100 mV (vs SHE) on the basis of the behavior of numerous mediators. The inability of most of these mediators to equilibrate with the tyrosyl radical supports the notion that the radical exists in an extremely protected hydrophobic pocket that prevents most radical scavengers from interacting with the radical, resulting in its unusual stability. The formal midpoint potential of the diiron clusters of the R2 protein was determined to be −115 ± 2 mV at pH 7.6 and 4 °C. This reduction is a two-electron transfer process, making the R2 protein the first of the nonheme diiron proteins not to stabilize a mixed valence intermediate at ambient temperature. The formal midpoint potential of the dinuclear iron centers is pH dependent, exhibiting a 30 mV/pH unit variance, which indicates that one proton is accepted from the solvent per two electrons transferred to the dinuclear iron center upon reduction. The midpoint potential of the site-directed mutant Y122F R2 protein was also investigated under the same conditions, and this midpoint potential was determined to be −178 mV, providing the first direct evidence that the presence of the Y122 residue modulates the redox properties of the diiron clusters. The redox potentials of both the wild type and Y122F proteins experience cathodic shifts when measured in the presence of azide or the R1 protein. For the latter, the midpoint potentials were determined to be −226 mV for the wild type protein and −281 mV for the Y122F mutant protein, representing a negative shift of over 100 mV for both proteins. These results indicate that the presence of the Y122 residue does not influence the effect of R1 binding, that the R1 protein preferentially binds the oxidized form of R2, and that the binding of R1 acts as a regulatory control mechanism to prevent unnecessary turnover of the dinuclear iron centers.

The enzyme ribonucleotide reductase (RNR)[1] catalyzes the reduction of ribonucleotides to their corresponding deoxyribonucleotides for DNA biosynthesis (Stubbe, 1990). The enzyme from *Escherichia coli* is composed of two proteins, R1 and R2, each of which is a dimer of two equivalent protomers (Thelander & Reichard, 1979). The R1 protein contains the binding sites for substrates, both purines and pyrimidines, and allosteric cofactors, along with redox active cysteines that are involved in substrate reduction (Mao et al., 1992a,b). The R2 protein contains two dinuclear iron centers and the catalytically essential tyrosyl radical (Lynch et al., 1989; Nordlund & Eklund, 1993).

The dinuclear iron centers of the R2 protein are antiferromagnetically coupled high-spin Fe(III) clusters (Atkin et al., 1973; Petersson et al., 1980), each containing a μ-oxo bridge (Sjöberg et al., 1982). The X-ray crystal structure of the R2 protein (Nordlund et al., 1990; Nordlund & Eklund, 1993) shows that the two diiron centers are located 25 Å apart in the R2 protein, with a separation of 3.3 Å between the two iron atoms in each center. The function of the dinuclear iron centers appears to be the generation and stabilization of the catalytically essential radical at Y122. The reaction of fully reduced R2 protein ($R2_{red}$) with oxygen engenders transient intermediates (Bollinger et al., 1991, 1994a,b; Ravi et al., 1994) that are directly involved in the generation of this radical. This Y122 radical is located 5.3 Å from the nearest iron atom of the center and is buried approximately 10 Å from the protein surface; this isolation may contribute to its unusual stability but also appears to prohibit its direct involvement in hydrogen abstraction from the substrate.

While a great deal of structure/function research has been conducted on R2, there has been little insight into the electron transfer processes associated with this protein. To date, the only information known about the redox properties of the dinuclear iron centers is an estimated redox potential range from −110 to +11 mV, based on the ability of several redox

† This work was supported by NIH Grant GM29344 (M.T.S.), NSF Grant MCB-9405723 (L.Q.), and the University of Minnesota Graduate School.

* Author to whom correspondence should be addressed. Tel.: (612) 624-1019. FAX: (612) 626-7541.

‡ Current address: Department of Chemistry, Hamilton College, Clinton, NY 13323.

® Abstract published in *Advance ACS Abstracts,* October 15, 1995.

[1] Abbreviations: E, measured equilibrium potential; E_m, formal midpoint potential value; $E^{\circ\prime}$, formal potential value; $E_m^{\circ\prime}$, formal midpoint potential value under set conditions; $E_1^{\circ\prime}$, formal potential value for the first electron transfer to the diiron cluster; $E_2^{\circ\prime}$, formal potential value for the second electron transfer to the diiron cluster; MCAD, medium chain acyl CoA dehydrogenase; MMO, methane monooxygenase; MMOB, MMO component B; MMOH, MMO hydroxylase component; MMOR, MMO reductase; n, number of electrons; RNR, ribonucleotide reductase; R1, the R1 protein of ribonucleotide reductase; R2, the R2 protein of ribonucleotide reductase; $R2_{ox}$, the R2 protein with the diiron(III) centers and the oxidized tyrosine; $R2_{met}$, the R2 protein with the diiron(III) centers and the reduced tyrosine; $R2_{red}$, the R2 protein with the diiron(II) centers and the reduced tyrosine; SHE, the standard hydrogen electrode.

0006-2960/95/0434-14093$09.00/0

mediators to reduce the cluster (Lam et al., 1990). While such an estimate is important, several factors were not addressed in that study. First, no actual thermodynamic measurements with an analysis of the reversibility of the process or the number of electrons transferred were obtained. Second, the range of −110 to +11 mV is very large for proteins. The actual potential could fall anywhere within this range. Third, the possibility that the redox potential value of the protein is influenced by pH, ionic strength, and temperature was not addressed. A more rigorous examination of the redox properties of the dinuclear iron centers is necessary to relate that information to the structure/function data available and for comparison to other nonheme dinuclear iron centered proteins for which such redox data already exists (Wang et al., 1991; Paulsen et al., 1994).

Along with understanding the course of electron transfer through the diiron clusters and how this transfer is affected by the environment, it is also important to understand what interactions may possibly control the potential of the iron centers. To accomplish this, we have used a spectroelectrochemical approach to investigate the effects of (a) the tyrosine 122 residue, (b) the binding of exogenous azide, and (c) the binding of R1 to R2 on the redox potential of the diiron cluster of R2.

EXPERIMENTAL PROCEDURES

Materials. R2 was isolated from *E. coli* strain N6405/pSPS2, a heat-inducible overproducer (strain provided by Dr. JoAnne Stubbe, M.I.T.). The purification and reconstitution of this protein was performed by the reported method (Lynch et al., 1989). Protein concentration was determined by the absorbance at 280 nm (ϵ = 141 mM^{-1} cm^{-1}) (Lynch et al., 1989). $R2_{met}$ was prepared as previously described (Lynch, 1989). Iron concentration was determined by the absorbance at 370 nm (ϵ = 8750 M^{-1} cm^{-1}) of the $R2_{met}$ form of the protein. The presence of a full complement of iron was determined from the ratio of the absorbances at 370 and 280 nm (0.065 ± 0.002) and by the ability of the fully reduced R2 protein to generate the maximum amount of tyrosyl radical (1.4 ± 0.1/protein) upon exposure to oxygen. The R2 protein isolated from five different preparations and used in these studies all satisfied the above criteria. In order to quantitate the tyrosyl radical concentration, the spectrum at 410 nm must be corrected for the absorption contribution of the dinuclear iron centers. In order to accomplish this, the iron absorption was estimated at 410 nm from the absorbances at 406 and 416 nm using data provided by Dr. M. Bollinger, Jr. ($\epsilon_{410\ \text{dropline}}$ = 1853 mM^{-1} cm^{-1} at 5 ± 1 °C), where the dropline value is calculated as $A_{410} - \{[3(A_{416} + 2(A_{406})]/5\}$ (Bollinger et al., 1991; Mao et al., 1992a).[3] This method has been confirmed in this laboratory using combined EPR and UV−Vis spectroscopy experiments. The procedure utilized to isolate the mutant Y122F protein from *E. coli* strain K38/pMK5/pGP1-2 (strain provided by Dr. B.-M. Sjöberg, University of Stockholm, Stockholm, Sweden) was identical to that of the wild type protein. R1 was the generous gift of Dr. Harry Hogenkamp, University of Minnesota.

The chemicals used and their sources as are follows: methyl viologen (British Drug House); riboflavin (Eastman Kodak); ferrocene monocarboxylic acid, 1,1′-dimethylferrocene, ferrocene-1,1′-dicarboxylic acid, glycerol, and HEPES [*N*-2-(hydroxyethyl)piperazine-*N*′-2-ethanesulfonic acid] (Aldrich); magnesium chloride [$MgCl_2$]; dithiothreitol [DTT]; phenosafranin, safranin O, chloramine-T, chloramine-B, Tris [tris(hydroxylmethyl)aminomethane]; MOPS [3-(*N*-morpholino)propanesulfonic acid], and MES [2-(*N*-morpholino)-ethanesulfonic acid] (Sigma); deuterium oxide [D_2O] (Isotec Inc.); Na_3IrBr_6, Na_3IrCl_6 (Alfa); tris(3,4,7,8-tetramethyl-1,-10-phenanthroline)iron(II) perchlorate, tris(4,4′-dimethyl-2,2′-bipyridine)iron(II) perchlorate, tris(2,2′-bipyridine)iron(II) perchlorate, tris(5-methyl-1,10-phenanthroline)iron(II) perchlorate, tris(1,10-phenenthroline)iron(II) perchlorate, tris-(5-nitro-1,10-phenanthroline)iron(II) perchlorate, and tris-(2,2′-bipyridine)ruthenium(II) dichloride (G. F. Smith); ferric sulfate (Mallinckrodt). 8-Chlororiboflavin was the generous gift of J. P. Lambooy, University of Maryland. Lumiflavin-3-acetate was the generous gift of Sandro Ghisla, University of Konstanz, Wester Germany. Water was glass-distilled.

Methods. Spectroelectrochemical Titrations. The spectroelectrochemical cell and the titration method have been previously described (Stankovich, 1980; Stankovich & Fox, 1983). All titrations were performed using 25 mM HEPES buffer containing 5% glycerol at pH 7.6 and 4 °C except for the pH study titrations in which conditions were as follows: 25 mM MES containing 5% glycerol at pH 6.2 and 4 °C; 25 mM MOPS containing 5% glycerol at pH 7.06 and 4 °C; 25 mM Tris containing 5% glycerol at pH 8.05 and 4 °C. The pH was determined before and after each experiment.

All spectrophotometric measurements were made using a Varian Cary 210 spectrophotometer with thermostated cell compartments. The spectra were recorded and stored on an Apple II+ or IIe computer. Potential measurements were made using either a BAS-100 electrochemical analyzer or an Orion Research model 601A digital ionalyzer. The equilibrium potential was determined to be stabilized when the measured potential changed by less than ±1 mV over a 10−15 min period. The reference electrode potential was determined using a standard solution of potassium ferricyanide and potassium ferrocyanide, each at a concentration of 50 mM in a 100 mM potassium phosphate buffer at pH 7.0 and 25 °C. The formal potential of this solution, under these conditions, is +425 mV versus the SHE (O'Reilly, 1973). The temperature dependence of the Ag/AgCl reference electrode formal potential was determined to be +4 mV on going from 25 to 4 °C. The method for measuring this potential difference has previously been reported (Stankovich & Fox, 1984).

The protein concentration for all experiments was 10−20 μM with a starting volume of 4−5 mL. The redox potential determination for R2 and Y122F with R1 used 10−20 μM R2 or Y122F, with 11−26 μM R1, and also contained 1 μM $MgCl_2$. These conditions were utilized based on the overall dissociation constant of 0.18 μM (Climent et al., 1992) and the assumption that a 1:1 mixture of R1 to R2 results in the formation of a complete complex. A 1.1−1.3 molar excess of R1 was used to ensure complete complex formation. The R1 protein was stored in 25 mM HEPES containing 5% glycerol and 100 μM DTT to ensure that the

[2] K. D. Burns, P. Pieper, H.-W. Liu, and M. T. Stankovich, unpublished results.

[3] The value reported here is slightly different than that reported in these references based on the data provided by Dr. M. Bollinger, Jr., which was obtained under the same conditions used for these experiments, and the correlation of data obtained in our lab with this reported value.

cysteine groups on the R1 protein were in the reduced form. For the azide experiments, the concentration of azide necessary to give a specific molar ratio of azide to iron was calculated from a stock solution of sodium azide. The appropriate volume of this stock was added to the protein solution immediately prior to degassing.

Methyl viologen was used to mediate electron transfer in the reductive direction for all electrochemical experiments. Ferrocenemonocarboxylic acid was used to mediate electron transfer in the oxidative direction. The concentration of methyl viologen (50−100 μM) was in excess of the diiron cluster concentration, while ferrocenemonocarboxylic acid and all redox indicators were used at a concentration of 2−4 μM. In order to determine whether the redox indicators bound to R2, different indicator mixtures were utilized for each redox potential determined. The ease of indicator spectrum subtraction, the use of indicator isobestic points, and the fact that the redox potentials of these dyes do not change in the presence of protein support the notion that these indicators do not bind to the diiron centers. Also, to minimize the effect of binding, the dyes used were at much lower concentrations than protein. Finally, all of these indicators, except for lumiflavin-3-acetate, phenosafranin, and safranin O, have previously been checked for binding with methane monooxygenase hydroxylase component (MMOH) by observing the EPR spectrum of the mixed valence form of the protein in the presence of each indicator to check for spectral perturbations (Paulsen et al., 1994). Since the diiron centers of MMOH are more accessible than the centers of R2, the lack of binding of these indicators with MMOH sets a precedent for their lack of binding with R2.

The midpoint potentials of the following redox indicators were determined by the spectroelectrochemical method under the same conditions used in this work (pH 7.6 and 4 °C): 8-chlororiboflavin ($E_m^{\circ\prime}$ = −107 mV); lumiflavin-3-acetate ($E_m^{\circ\prime}$ = −198 mV); riboflavin ($E_m^{\circ\prime}$ = −174 mV); phenosafranin ($E_m^{\circ\prime}$ = −237 mV); and safranin O ($E_m^{\circ\prime}$ = −298 mV). The midpoint potentials for methyl viologen ($E^{\circ\prime}$ = −450 mV), ferrocenemonocarboxylic acid ($E^{\circ\prime}$ = +590 mV) (Wilkinson et al., 1952), Na_3IrBr_6 ($E^{\circ\prime}$ = +800 mV), Na_3IrCl_6 ($E^{\circ\prime}$ = +910 mV) (DeFelippis et al., 1989), and hydroxyurea ($E^{\circ\prime}$ = +724 mV) (Lam et al., 1990) were measured at pH 7.0 and 25 °C. The redox potentials for tris(3,4,7,8-tetramethyl-1,10-phenanthroline)iron(II) perchlorate ($E^{\circ\prime}$ = +810 mV), tris(4,4′-dimethyl-2,2′-bipyridine)-iron(II) perchlorate ($E^{\circ\prime}$ = +950 mV), tris(2,2′-bipyridine)-iron(II) perchlorate ($E^{\circ\prime}$ = +970 mV), tris(5′-methyl-1,10-phenanthroline)iron(II) perchlorate ($E^{\circ\prime}$ = +1020 mV), tris(1,10-phenanthroline)iron(II) perchlorate ($E^{\circ\prime}$ = +1060 mV), tris(5-nitro-1,10-phenanthroline)iron(II) perchlorate ($E^{\circ\prime}$ = +1250 mV), and tris(2,2′-bipyridine)ruthenium(II) dichloride ($E^{\circ\prime}$ = +1330 mV) (G. F. Smith) were determined at 25 °C in acetonitrile. All redox potentials are reported versus the standard hydrogen electrode (SHE).

D_2O Experiments. Experiments to investigate possible hydrogen-bonding interactions were conducted in D_2O and utilized similar protein, indicator, and mediator concentrations as in the H_2O experiments. All solutions were made with fresh D_2O and kept desiccated. The electrodes used in the spectroelectrochemical cell also contained D_2O solutions. The reference and auxiliary electrodes contained 1.0 M KCl to overcome the overpotential caused by the 23% higher viscosity of D_2O (Walsh, 1979) versus the 0.1 M KCl concentrations used with glass-distilled water. The pD of the solutions was determined using the formula pH = pD + 0.4 (Walsh, 1979).

The appropriate volume of protein was dialyzed versus the D_2O solution for 2 days with three changes in dialysis buffer in an attempt to obtain complete deuterium exchange. The time of each dialysis was closely controlled to prevent differences in the amount of exchange that was obtained. All dialyzed protein solutions and deuterium solutions were freshly prepared.

The redox indicators utilized for these experiments were prepared in fresh D_2O solutions. In order to determine the deuterium isotope effect upon these reagents, their midpoint potentials were determined in D_2O under the same conditions used for the protein experiments. The midpoint potentials determined are as follows: 8-chlororiboflavin ($E_m^{\circ\prime}$ = −138 mV), riboflavin ($E_m^{\circ\prime}$ = −216 mV), and lumiflavin-3-acetate ($E_m^{\circ\prime}$ = −216 mV). The negative shift in potential for all of these indicators is largely due to their proton dependence.

Tyrosyl Radical Potential. These experiments involved the addition of a mediator to a solution of the $R2_{ox}$ protein and then monitoring the absorbance of the radical over time. The experiments were performed sequentially, with the radical being incubated with a more positive potential mediator in each successive experiment to determine if that mediator could reduce the radical. Incubations over extended time periods were conducted at 4 °C with stirring.

More positive mediators were tested via the spectroelectrochemical method. Experiments were conducted in both the oxidative and reductive directions. The ability of the mediator to oxidize, reduce, or equilibrate with the radical was investigated.

Calculations. The electron inventory of the dinuclear iron centers for each protein was determined using the following equation:

$$\Delta Q = nFN \tag{1}$$

where Q is the number of coulombs used to reduced the protein, n is the number of electrons transferred to the protein throughout the reduction, F is the Faraday's constant (96 487 mC/mmol of electrons), and N is the number of moles of the protein in solution, calculated from the absorbance of the solution at 280 nm and also at 370 nm. The electron inventory for the tyrosyl radical was determined using the same equation, with the number of moles of radical present determined by the method provided by Dr. M. Bollinger, Jr., mentioned earlier. The methodology utilized for these determinations currently exhibits a 94%−98% efficiency.

The midpoint potentials (E_m) and n values were calculated by a computerized nonlinear regression fit (Duggleby, 1981) to a plot of E versus [ox]/[red] using the Nernst equation

$$E = E_m + (0.059/n)\log([ox]/[red]) \tag{2}$$

where E is the measured equilibrium potential at each point in the titration and n is the number of electrons. In determining the final reported midpoint potential under a specified condition, the results of several experiments were incorporated together and included in the nonlinear regression analysis. The uncertainty value for the reported midpoint potentials is ±1−3 mV and is calculated through the computerized nonlinear regression analysis. All midpoint potential values exhibited Nernstian behavior as demonstrated by their n values which are calculated from the slopes of the Nernst plots.

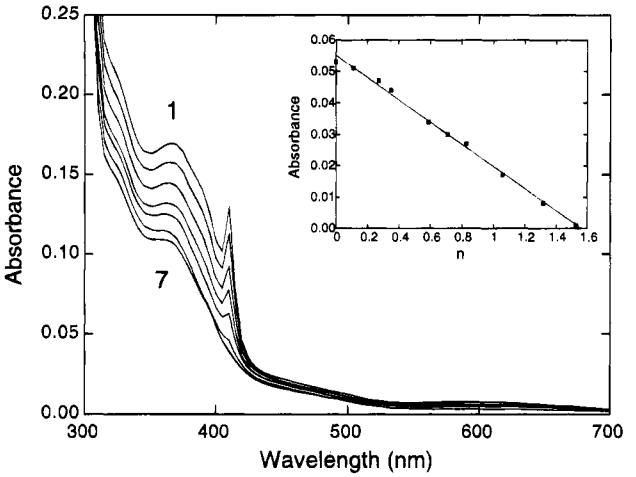

FIGURE 1: Coulometric reduction of $R2_{ox}$ (20 μM) with 100 μM methyl viologen and 2 μM 8-chlororiboflavin in 25 mM HEPES buffer (pH 7.6) containing 5% glycerol at 4 °C (curves 1−7; n = 0.0, 0.27, 0.59, 0.83, 1.06, 1.32, and fully reduced, respectively). The inset shows the decrease in the absorbance at 410 nm (see Materials and Methods for description of dropline quantitation procedure) as a function of reducing equivalents added (n).

The binding constant for the reduced R1−R2 complex and the binding constant ratio for the addition of azide were determined from the relationship of binding constants to midpoint potentials, assuming saturating conditions, using the following equation:

$$E_{bound} = E_m - (0.054/n)\log K_{d2}/K_{d1} \quad (3)$$

which has been reported previously (Clark, 1960; Einarsdottir et al., 1989).

RESULTS

Quantitation and Midpoint Potential of the Tyrosyl Radical. Active RNR contains two redox centers: the Y122 radical and the diiron(III) center. Before discussing the redox chemistry of the diiron center in detail, the results of our studies on the radical will be presented. The coulometric reduction of the tyrosyl radical is shown in Figure 1. Quantitation of the radical absorption feature at 410 nm shows that a total of 1.4 ± 0.1 radicals per protein are present. This agrees well with previously published results (Lynch et al., 1989). This value was confirmed using three different preparations of the protein. Complete reduction of the protein to $R2_{red}$ followed by reoxidation again generates 1.4 ± 0.1 tyrosyl radicals/protein.

When the reduction of the radical is stopped after the disappearance of the radical peak at 410 nm and the protein is reoxidized with oxygen, a small amount of radical is regenerated. This implies that some reduction of the dinuclear iron center occurs before the entire tyrosyl radical is reduced, since radical generation can only occur through the reaction of the reduced diiron center with oxygen. Three explanations can account for such an observation. First, the redox potential of the radical may be only slightly more positive than that of the dinuclear iron centers. Since radicals are believed to have very positive redox potentials (DeFelippis et al., 1989), this explanation did not seem plausible. Secondly, the dinuclear iron centers may serve as the conduit for the reduction of the tyrosyl radical under anaerobic conditions. This situation may arise if the dinuclear iron centers are more accessible to the electrochemical reductant than the radical. Such a mechanism may require a transient mixed valance form of the diiron center. While transient mixed valance intermediates have been postulated previously (Nordlund, 1990), the redox properties of such a mechanism have not been elucidated to date. Third, the reduction of the radical may be kinetically slow. In order to determine which situation applied, the coulometric titrations were carried out in the presence of 8-chlororiboflavin, a redox indicator with a potential (−107 mV) similar to that of the diiron centers (vide infra). In the first case, this indicator would have no effect. In the latter case, the 8-chlororiboflavin would be reduced before the diiron centers and thus prevent the reduction of the diiron centers prior to complete reduction of the tyrosyl radical. In the presence of 8-chlororiboflavin the complete reduction of the tyrosyl radical was possible without the regeneration of any radical upon exposure to oxygen. This indicates that the iron centers were not reduced and that the redox potential of the radical is not similar to that of the diiron center. At this point, we can not distinguish between the other two possibilities. In order to achieve the correct absorption spectrum of the radical (Figure 1), the absorption spectrum of 8-chlororiboflavin was subtracted from all of the tyrosyl radical reduction spectra.

The midpoint potential of the tyrosyl radical was investigated in both the reductive and oxidative directions. The redox indicators utilized in these experiments and their interaction with the radical are listed in Table 1. 1,1′-Dimethylferrocene and ferrocene were able to reduce the tyrosyl radical, but only after overnight incubation with the protein. Ferrocenemonocarboxylic acid and 1,1′-ferrocenedicarboxylic acid were able to cause a very slight reduction of the radical upon overnight incubation. These results indicate that the redox potential for the tyrosyl radical is more positive than +644 mV, in agreement with reduction of the radical by hydroxyurea, which has a redox potential of +727 mV. The ability of tris(2,2′-bipyridine)ruthenium(III) dichloride to oxidize Y122 to its radical a small extent demonstrates that the redox potential for the radical is more negative than +1330 mV.

The remaining redox indicators could neither reduce, oxidize, or equilibrate with the tyrosyl radical, even during overnight incubation, indicating that these indicators cannot penetrate the protein to reach the tyrosyl radical for equilibration. Therefore, a successful determination of the equilibrium potential for the tyrosyl radical could not be obtained through the spectroelectrochemical method. The ability to work in the oxidative direction was prohibited by the generation of oxygen in the electrodes of the spectroelectrochemical cell at potentials greater than the potential for the oxidation of water to oxygen (+787 mV at pH 7.5). On the basis of results obtained, the reduction of the radical appears to occur as shown in eq 4, with an apparent redox

$$Y122^{\bullet}\,(R2_{ox}) + e^- + H^+ \rightleftharpoons Y122\,(R2_{met}) \quad (4)$$

potential of +1000 ± 100 mV.

Quantitation and Midpoint Potentials of $R2_{met}$. A coulometric reduction of $R2_{met}$ shows the characteristic spectrum exhibited by the dinuclear iron centers upon reduction (Figure 2). Quantitation of the results based on the absorption of the diiron centers, the absorption at 280 nm, and the average of these values determined from several separate experiments shows that 3.9 ± 0.2 reducing equiv are necessary for full reduction, in good agreement with the established Fe:R2

Table 1: Mediators Used in the Estimate of the Tyrosyl Radical Redox Potential and Their Effect on the Radical

compound	$E^{\circ\prime}$(V)	effect on radical
1,1′-dimethylferrocene	+0.341	reduced overnight
ferrocene	+0.422	reduced overnight
ferrocenemonocarboxylic acid	+0.530	partial reduction overnight
1,1′-dicarboxylic acid ferrocene	+0.644	partial reduction overnight
hydroxyurea	+0.724	reduced
$IrBr_6^{3-}$	+0.800	could not oxidize
$IrCl_6^{3-}$	+0.910	could not oxidize
tris(3,4,7,8-tetramethyl-1,10-phenanthroline)iron(II) perchlorate	+0.810	no equilibration
tris(4,4′-dimethyl-2,2′-bipyridine)iron perchlorate	+0.950	no equilibration
tris(2,2′-bipyridine)iron(II) perchlorate	+0.970	no equilibration
tris(5-methyl-1,10-phenanthroline)iron(II) perchlorate	+1.020	no equilibration
tris(1,10-phenanthroline)iron(II) perchlorate	+1.060	no equilibration
tris(5-nitro-1,10-phenenthroline)iron(II) perchlorate	+1.250	no equilibration
tris(2,2′-bipyridine)ruthenium(II) dichloride	+1.330	slight oxidation
chloramine-T	+0.900	no equilibration
chloramine-B	+0.900	no equilibration

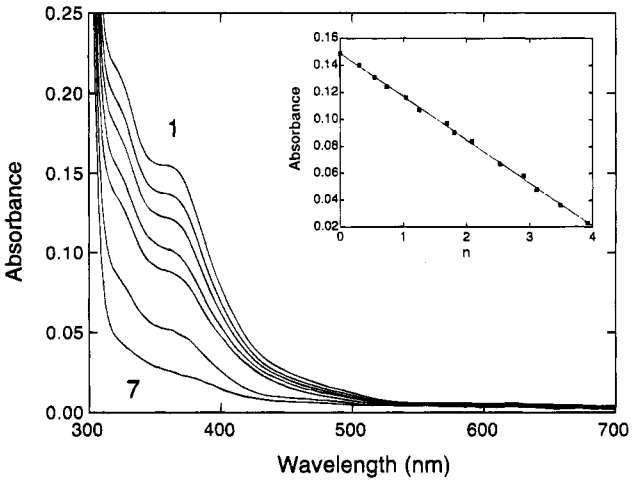

FIGURE 2: Coulometric reduction of $R2_{met}$ (17 μM) with 100 μM methyl viologen in 25 mM HEPES buffer (pH 7.6) containing 5% glycerol at 4 °C (curves 1−7; n = 0.0, 0.55, 1.04, 1.69, 2.09, 3.11, and fully reduced, respectively). The inset shows the decrease in absorbance at 370 nm as a function of the number of reducing equivalents added (n).

Table 2: Midpoint Potential of $R2_{met}$ at Various pH Values

pH	6.22	7.07	7.61	8.05
E_m (mV)	−72	−94	−115	−127

stoichiometry (Lynch et al., 1989; Norlund & Eklund, 1993). No change in the visible spectrum or deviation from the coulometric reduction plot is observed during the reduction, suggesting that a mixed valence form of the protein is not formed. The addition of oxygen to the fully reduced $R2_{met}$ protein results in the generation of the spectrum associated with the native protein. Quantitation of the tyrosyl radical shows that the maximum amount of radical (1.4 ± 0.1/protein) is restored upon oxidation, demonstrating that there was complete occupation of the iron sites in the protein.

The midpoint potentials of the dinuclear iron center were determined from pH 6.2 to 8.05, the range over which stable potential measurements could be determined. These data are summarized in Table 2. Numerous midpoint potential titrations were conducted at pH 7.6. Under these conditions the midpoint potential of the dinuclear iron centers was determined to be −115 mV. These results are shown in Figure 3. This potential was independent of different preparations of the HEPES buffer, different indicators, and different concentrations of indicator. The calculated n value

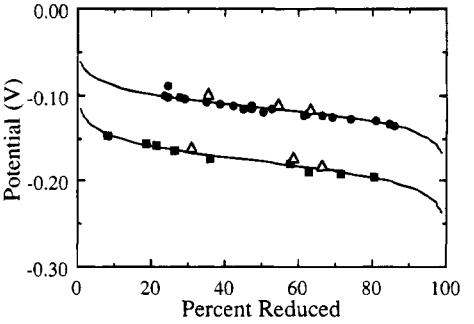

FIGURE 3: Midpoint potential titrations for 20 μM $R2_{met}$ and Y122F at pH 7.6. Simulations of the percent reduced for $R2_{met}$, E_m = −115 mV, and Y122F, E_m = −178 mV, are shown as solid lines. The individual data points for $R2_{met}$ (●) and Y122F (■) are shown. Experimental points obtained in the oxidative direction (△) are also displayed. The data from three to six experiments are contained in the plots.

Table 3: Midpoint Potentials and Nernstian Slopes for the Reduction of $R2_{met}$, Y122F, and Their Respective Indicators at pH (pD) 7.6.

	in water		in D_2O	
sample	E_m (mV)	slope (mV)	E_m (mV)	slope (mV)
$R2_{met}$	−115	26	−200	26
Y122F	−178	31	−207	32
8-chlororiboflavin	−107	37	−138	29
riboflavin	−174	34	−216	25
lumiflavin-3-acetate	−198	26	−216	27

from these experiments shows that the reduction occurs via a two-electron transfer process. This agrees well with Nernstian analysis that results in a slope of 26 mV, indicative of a two-electron transfer at pH 7.6 (Table 3). The midpoint potentials vary as a function of pH with a value of 30 mV/pH unit (Figure 4). Based on the pH dependence of the Nernst equation, this predicts that one proton from solvent accompanies two electrons during the reduction of one dinuclear iron center. Therefore, according to our redox data, the reduction for one dinuclear iron center proceeds as in eq 5.

$$\text{Fe(III)Fe(III)}\ (R2_{met}) + 2e^- + 1H^+ \rightleftharpoons \text{Fe(II)Fe(II)}\ (R2_{red}) + OH^- \quad E_m = -115\ \text{mV} \quad (5)$$

Reversibility was tested by using ferrocene monocarboxylic acid to mediate electron transfer in the oxidative direction. The protein was partially reduced, and a potential measure-

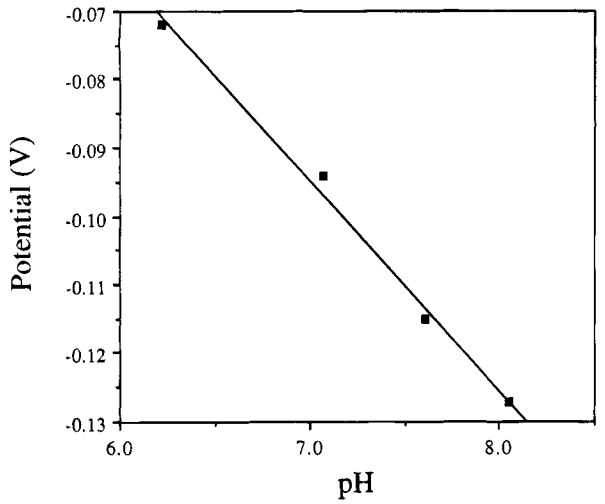

FIGURE 4: Plot of the midpoint potential for the dinuclear iron clusters of $R2_{met}$ as a function of pH.

ment was carried out. The protein was then partially oxidized, and the equilibrium potential was again determined. This process was repeated throughout the titration. The positive change in potential along with the increase of absorbance of the dinuclear iron band indicated that the centers were being reoxidized. In addition, the points obtained in the oxidative direction fall on the same Nernst plot as the data collected in the reductive direction, as indicated in Figure 3.

Quantitation and Midpoint Potential for Uncomplexed Y122F R2. A coulometric titration of the mutant Y122F protein shows the identical spectrum exhibited by the wild type $R2_{met}$ protein (Figure 5). Quantitation of the results by the same method used with the WT $R2_{met}$ protein shows that 3.9 ± 0.2 reducing equiv are necessary for full reduction of the protein. The addition of oxygen to the fully reduced protein completely restores the spectrum of oxidized Y122F R2.

The midpoint potential of the dinuclear iron centers, determined under the conditions used for the wild type protein (pH 7.6), was established to be −178 mV. The *n* value determination and Nernstian analysis (slope of 31 mV, Table 3) also led to the conclusion that this is a two-electron transfer. Thus, the reduction occurs via eq 6,with the same

$$\text{Fe(III)Fe(III) (Y122F R2}_{ox}) + 2e^- + 1H^+ \rightleftharpoons$$
$$\text{Fe(II)Fe(II) (Y122F R2}_{red}) + OH^- \quad E_m = -178 \text{ mV} \quad (6)$$

protonation mechanism as the WT protein. The comparison of the redox potentials for the wild type protein and the Y122F protein is shown in Figure 3. The large negative shift in the midpoint potential of the Y122F protein was surprising due to the identical diiron center spectral features observed for the two proteins (Elgren et al., 1991). Reversibility was also confirmed on this protein by the same method used with the wild type protein. Along with the large difference in the midpoint potential between the two proteins, there was a drastic change in the kinetic range of reduction for the Y122F protein. The reduction proceeds normally for approximately the first half of the reduction and then becomes increasingly more difficult as the reduction progresses.

Midpoint Potentials of Wild Type and Y122F $R2_{met}$ in D_2O. On the basis of the unexpected negative shift in the midpoint

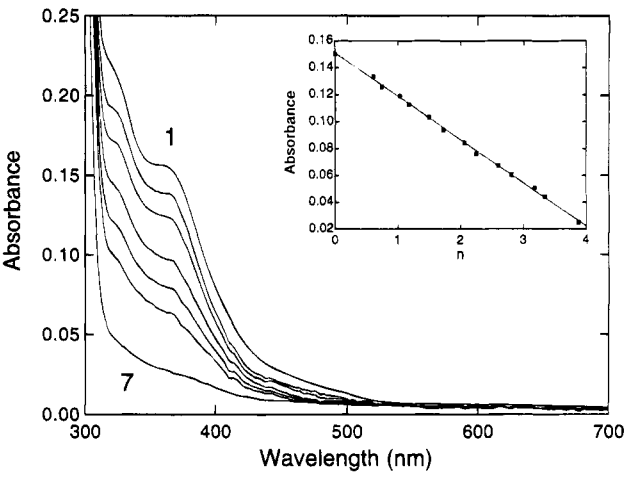

FIGURE 5: Coulometric reduction of Y122F (17 μM) with 100 μM methyl viologen in 25 mM HEPES buffer (pH 7.6) containing 5% glycerol at 4 °C (curves 1−7; $n = 0.0$, 0.61, 1.03, 1.72, 2.25, 2.81, and fully reduced, respectively). The inset shows the decrease in absorbance at 370 nm as a function of reducing equivalents added (n).

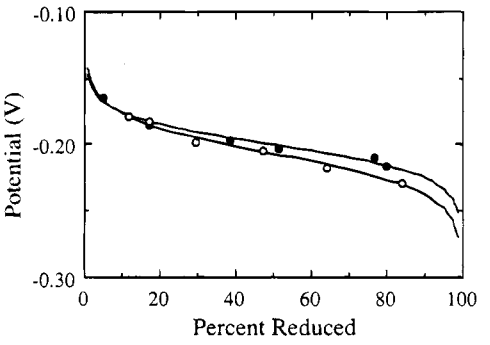

FIGURE 6: Midpoint potential titrations for 20 μM $R2_{met}$ and Y122F in D_2O at pD 7.6. Simulations of the percent reduced for $R2_{met}$, $E_m = -200$ mV, and Y122F, $E_m = -207$ mV, are shown as solid lines. The individual data points for $R2_{met}$ (●) and Y122F (○) are shown.

potential of the Y122F protein, the midpoint potentials for the two proteins were determined in D_2O to investigate the possibility that a specific hydrogen-bonding interaction modulates the redox potential of the dinuclear iron center. Conditions were kept identical to the experiments conducted in water. The midpoint potentials for the $R2_{met}$ and Y122F proteins (Figure 6) were determined to be −200 and −207 mV, respectively. The overall reduction equations would be identical to the above reactions in H_2O, expect for the substitution of deuterium ions for the protons. The midpoint potentials for the redox indicators were also measured in D_2O to determine the solvent-induced effect of deuterium substitution of these chemicals. All results are summarized in Table 3.

In contrast to their behavior in water, both proteins exhibited similar reduction characteristics in D_2O. First, the equilibrium of both proteins was much slower in D_2O than in water. Second, both reductions still occur via a two-electron transfer mechanism, and, most surprising, the reduction potentials of both proteins are approximately the same (Table 3) in D_2O. Thus it appears that the D_2O exchange has a larger effect upon the proteins than can be explained by a specific hydrogen-bonding interaction.

Midpoint Potentials in the Presence of Azide. Azide, at high concentrations, has been shown to bind to $R2_{red}$ (Elgren et al., 1993); thus the redox chemistry of R2 was investigated

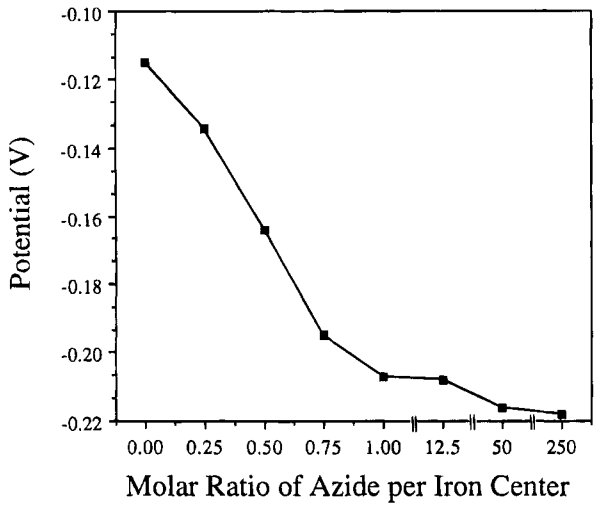

FIGURE 7: Plot of the midpoint potential for the dinuclear iron centers of $R2_{met}$ versus the molar ratio of azide to iron content.

in the presence of azide. Interestingly, the results for the midpoint potential determinations in the presence of increasing azide are shown in Figure 7, represented as the midpoint potential versus the molar ratio of azide to iron centers. The addition of substoichiometric amounts of azide results in a negative shift in the midpoint potential of the dinuclear iron centers. The midpoint potential continues to decrease until the ratio of azide to protein is approximately one azide molecule to one iron center, where the potential levels off at approximately −207 mV. The addition of a large excess of azide (250 molar excess) is necessary to cause a further decrease in the diiron midpoint potential, but results in only an additional 11 mV negative shift to −218 mV. Experiments with very high azide concentrations could not be conducted because the azide removed the iron from the protein. Under these conditions, the measured potential simply continued to spiral more positive and would not stabilize. Furthermore, the behavior of the reduction in the presence of high azide concentrations became non-Nernstian. The formation of an free iron azide complex in solution is further evidenced by the growth of an absorption band in the region 410−430 nm. The longer the azide is present in solution with the $R2_{met}$ protein, the more this absorption band develops. The potentials reported here allowed for incubation of azide with $R2_{met}$ for up to 12 h before iron removal was evidenced. This time frame allowed for stabilized equilibrium potentials (10−15 min) and the collection of adequate data points to determine the redox potential of the dinuclear iron centers.

Several control experiments were carried out to ensure that the negative shift in midpoint potential was truly the result of azide binding to the diiron centers of R2 and not due to a change in ionic strength or the result of an iron−azide complex. For the ionic strength control, the experiment was carried out in the presence of a large excess of NaCl (25 molar excess), and the midpoint potential was determined to be −131 mV. In another experiment, a solution of azide with ferric sulfate at pH 7.6 was titrated, and several experiments afforded equilibrium potentials in the +300 mV region, showing that an unbound iron−azide complex exhibits a much more positive potential than is observed when azide is incubated with the $R2_{met}$ protein. On the basis of spectral evidence, however, the removal of iron from the centers by azide occurs for both the oxidized and reduced forms of the protein; this was not evident until after 12 h. All the experiments at lower azide concentrations were completed in 8−10 h. These experiments show that the negative shift in the midpoint potential in the presence of azide is definitely due to the binding of azide to the dinuclear iron centers.

The reversibility of these azide experiments was investigated using the same procedure developed for the $R2_{met}$ protein. The midpoint potentials determined in the reductive and oxidative direction differ by 59 mV (−186 and −127 mV at 25 molar excess of azide for the reductive and oxidative directions, respectively). The difference in the reductive potentials of −207 and −186 mV is possibly due to the dissociation of azide, where the dissociation of azide is comparable to the rate of reduction. This is supported by the observation that the large difference between the reductive and oxidative titrations shows a preferential binding of azide to one redox form of the dinuclear iron centers. Since the redox potential in the reductive direction is more negative than the potential in the oxidative direction, we propose that in these equilibrium experiments the reduction in the presence of azide proceeds by eq 7.

$$\text{Fe(III)Fe(III)}\ (R2_{met}{-}N_3^-) + 2e^- + 1H^+ \rightleftharpoons \text{Fe(II)Fe(II)}\ (R2_{red}) + N_3^- + OH^- \quad E_m = -207\ \text{mV} \quad (7)$$

The effect of azide on the midpoint potential of the mutant Y122F was also explored to determine if the same degree of potential shift was exhibited as in the wild type $R2_{met}$ protein. The determination of the midpoint potential under the same ratio of azide to iron that resulted in a midpoint potential of −207 mV in the wild type protein (25 molar excess) resulted in a midpoint potential of −252 mV for the mutant protein or a shift of −74 mV as compared to a potential shift of −93 mV for the wild $R2_{met}$ protein. Therefore, even though the degree of negative shift is slightly less than that exhibited in the wild type protein, the overall effect of azide addition is comparable.

Midpoint Potentials for Wild Type and Y122F $R2_{met}$ Bound to R1. The midpoint potential values for the wild type $R2_{met}$ and Y122F proteins while bound to the R1 protein were determined to be −226 and −281 mV, respectively. These results are shown in Figure 8. This negative shift can be attributed solely to the binding of R1 since the midpoint potential for the $R2_{met}$ protein was the same under the conditions used for these experiments. The negative potential shift induced by R1 binding is essentially the same for both proteins (−111 and −103 mV for $R2_{met}$ and Y122F, respectively). The calculated n values from these experiments show that the reduction of the dinuclear iron centers is also a two-electron transfer process in the presence of R1 which follows eqs 8 and 9.

$$\text{Fe(III)Fe(III)}\ (R1{-}R2_{met}) + 2e^- + 1H^+ \rightleftharpoons \text{Fe(II)Fe(II)}\ (R1{-}R2_{red}) + OH^- \quad E_m = -226\ \text{mV} \quad (8)$$

$$\text{Fe(III)Fe(III)}\ (R1{-}Y122F\ R2_{ox}) + 2e^- + 1H^+ \rightleftharpoons \text{Fe(II)Fe(II)}\ (R1{-}Y122F\ R2_{red}) + OH^- \quad E_m = -281\ \text{mV} \quad (9)$$

The binding of R1 to the wild type $R2_{met}$ and Y122F proteins does not change the visible spectrum of the respective proteins, indicating that the binding of R1 does

not significantly affect the structure of the dinuclear iron center. The addition of oxygen to the wild type $R2_{red}$ bound to R1 system results in the generation of the characteristic spectrum of the native R2 protein. The quantitation of the tyrosyl radical demonstrates that the maximum amount of radical can be restored. Therefore, the binding of R1 does not interfere with the generation of the tyrosyl radical or the oxidized spectrum of the dinuclear iron centers. Reoxidation of the mutant Y122F protein results in the regeneration of the fully oxidized Y122F spectrum, showing again that R1 binding does not interfere with the oxidation of the diiron centers.

DISCUSSION

We report here the first complete redox study of the R2 protein of ribonucleotide reductase from *E. coli*. A previous study on the R2 protein was unsuccessful in quantitating the number of reducing equivalents necessary for full reduction of the $R2_{met}$ and native forms of this protein (Sahlin et al., 1989). The results presented here provide the first reductive quantitation that supports the existence of two dinuclear iron centers, in agreement with the X-ray crystal structure (Nordlund & Eklund, 1993).

Our studies on the active form of the R2 protein first focused on the quantitation of the tyrosyl radical and its redox potential. While a constant value of 1.4 ± 0.1 radicals is reported for each experiment, the interesting observation is that the radical is not fully reduced before reduction of the dinuclear iron centers commences. It is therefore possible that, under anaerobic conditions, the dinuclear iron centers are reduced before or concurrently with the radical and may aid in the reduction of the radical. The addition of an indicator prevents any overreduction of the diiron centers and allows for the spectrum of $R2_{met}$ to be obtained, not the spectrum of partially reduced $R2_{met}$.

While the exact redox potential of the tyrosyl radical was not determined, these results provide an estimate of the potential of the radical. This estimate ($E^{o\prime} = +1000 \pm 100$ mV) also places the redox potential for the tyrosyl radical in the range of the tyrosine side chain neutral phenoxy radical, +940 mV at pH 7.0 (DeFelippis et al., 1989). These observations also agree with the structural evidence that the tyrosyl radical exists in a protected hydrophobic pocket that contributes to its unusual stability (Stubbe, 1990; Nordlund & Eklund, 1993; Ormö et al., 1995). The inability of most of these mediators to equilibrate with the radical combined with the conclusions based upon the reduction of this radical by methyl viologen suggests that only very small reductants can penetrate the protective environment of this radical.

From the X-ray crystal structure of the reduced S211A R2 protein (see Figure 9) (Åberg, 1993) it is observed that the following changes occur during reduction of the dinuclear iron centers. First, the μ-oxo bridge is lost by its protonation to water. Second, the endogenous iron carboxylate ligands undergo rearrangement; most noticeably, E238 converts to a bridging ligand and the two remaining terminal carboxylates become unsymmetrically chelated to their respective irons to make the diiron site more symmetrical. Third, the two water molecules coordinated to the irons in the oxidized form appear to be lost and a hydrogen bond is formed between Y122 and the iron ligand D84 (Åberg, 1993). Our data, as discussed below, supports several of these observations.

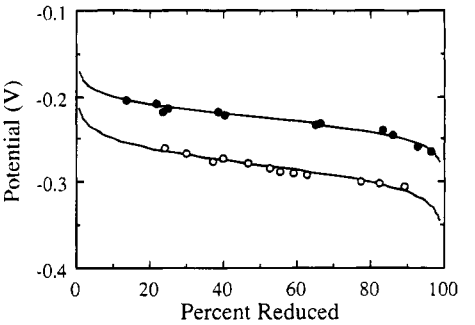

FIGURE 8: Midpoint potential titrations for 10−20 μM $R2_{met}$ and Y122F at pH 7.6 with 11−26 μM R1. Simulations of the percent reduced for $R2_{met}$, $E_m = -226$ mV, and Y122F, $E_m = -281$ mV, are shown as solid lines. The individual data points are shown for $R2_{met}$ (●) and Y122F (○) are shown.

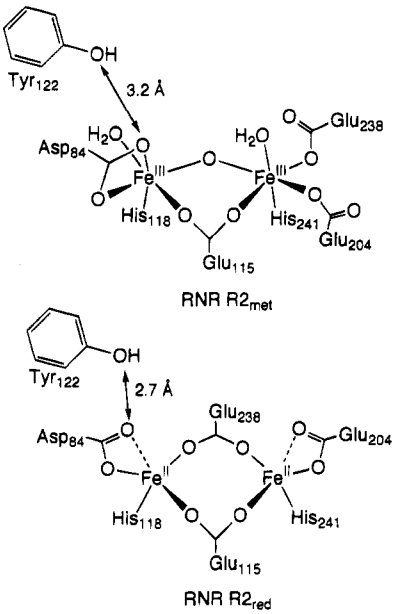

FIGURE 9: Diiron site structures of wild type $R2_{met}$ and S211A $R2_{red}$ [adapted from Atta et al. (1992) and Åberg (1993)].

The midpoint potential determination of −115 mV for the dinuclear iron centers at pH 7.6 is in good agreement with the initial range of ≥−110 mV determined by the reduction of the protein by several redox indicators (Lam et al., 1990). The agreement of these potentials is significant in that the experiments were conducted using protein isolated from different overproducing strains of *E. coli* and purified in different laboratories. The Nernstian behavior of this reduction potential explains several questions about this protein that to date have remained unanswered. First, the determination that the electron transfer to the dinuclear iron centers is via a two-electron transfer demonstrates that the two diiron centers each accept two electrons and react independently with the electrochemical reductant. Secondly, this two-electron transfer explains why no mixed valence state of the $R2_{met}$ protein has been observed in room temperature chemical reductions (Sahlin et al., 1989). In only three instances has a mixed valence form been observed in R2, once in the reduction of $R2_{met}$ with hydrazine (Gerez et al., 1991), which may bind to the diiron center, thus making this species a perturbed reductive intermediate, and the other two instances with low-temperature X- or γ-irradiation (Hendrich et al., 1991; Davydov et al., 1994). The fact that extraordinary conditions must be employed to produce a mixed valence intermediate demonstrates that this species

is not thermodynamically favored under normal conditions. The two-electron transfer exhibited by the protein in our experiments shows that the redox potential of the first electron ($E_1°'$) is much more negative than that of the second electron ($E_2°'$), making the transfer appear to be a simultaneous two-electron reduction. For proteins with nonheme diiron centers where a mixed valence state is formed, $E_1°'$ is more positive than $E_2°'$, allowing for reduction of the first iron to occur before the reduction of the second iron atom commences (Paulsen et al., 1994). The two-electron transfer of R2 may also help to explain the thermodynamic properties of the protein. It signifies that only two states of the dinuclear iron centers are readily stabilized *in vivo*, fully oxidized, which stabilizes the tyrosyl radical, and fully reduced, which generates this radical upon exposure to dioxygen. This also agrees with the observed regulation of the redox states of MMOH (Paulsen et al., 1994). In this system, the uncomplexed MMOH stabilizes approximately 60% mixed valence intermediate during reduction. However, the addition of the reductase component of MMO (MMOR) resulted in the formation of the diiron(II) form of MMOH upon reduction, with little mixed valence species observed. For MMOH it has been shown that only the two-electron reduced species interacts with dioxygen. Therefore, it appears that the ability of these diiron proteins to quantitatively form their fully reduced dinuclear iron centers is a key feature of their interaction with dioxygen. The formation of the mixed valence state in both cases would then be an inefficient step in the catalytic turnover of the protein. Since the principal function of the R2 protein seems to be the stabilization and regeneration of the catalytically essential tyrosyl radical, the ability to directly form the fully reduced protein assures efficient turnover of the dinuclear iron centers and regeneration of this radical.

The midpoint potential of the dinuclear iron center also supports the structural models proposed for similar centers. The more negative redox potential of R2 (−115 mV) versus uteroferrin (E_m = +367 mV) (Wang et al., 1991) and MMOH (E_m = +48 mV) (Paulsen et al., 1994) follows the hypothesis that the redox potential of a dinuclear iron center is dependent upon the number of oxygen ligands and the protonation state of the oxygen bridge. While all three proteins contain an oxygen-rich environment, the protonation state of the bridge differs in the three. The more positive reduction potentials for uteroferrin and MMOH support the existence of a hydroxo bridge. Evidence of this bridging ligand for MMOH and uteroferrin has been provided by ENDOR studies on the mixed valence states (DeRose et al., 1993; Thomann et al., 1993). The more negative redox potential of the dinuclear iron centers of R2 is consistent with an unprotonated bridge combined with an oxygen-rich ligand environment as shown in the X-ray crystal structure (Nordlund & Eklund, 1993).

The pH dependence exhibited by the dinuclear iron centers of R2 clearly show that one proton is transferred from the solvent concurrent with two electrons. However, two protons are needed to protonate the μ-oxo bridge upon reduction (Figure 9). There are two possible explanations for the observed single protonation. First, the second proton could come from a residue within the protein, perhaps through a proton shuttle mechanism from an outer sphere residue. Second, during reduction, the first proton may transfer to the oxo bridge, followed by the conformational change that occurs upon reduction. The second proton may transfer after this conformational change. This could place the protein in a metastable state during our equilibrium experiments that prevents the second proton transfer from being observed.

Table 4: Summary of the Redox Potentials and Potential Shifts for the Wild Type and Y122F $R2_{met}$ Proteins[a]

condition	E_m for WT R2	E_m for Y122F R2	ΔE WT-Y122F
in H_2O	−115	−178	63
in D_2O	−200	−207	7
+ azide	−207	−252	45
+ R1	−226	−281	65

[a] All values in mV.

The studies on the mutant protein Y122F demonstrate that it accepts the same number of reducing equivalents and exhibits the identical spectrum as the WT protein but there is a significant difference in the midpoint potentials between the two proteins. This may point to a structural difference between the two. The X-ray crystal structure of the reduced form of the R2 protein (Åberg, 1993) suggests evidence of a hydrogen bond between tyrosine 122 and aspartic acid 84, an iron ligand (Figure 9). This hydrogen bond is not found in the oxidized form of the dinuclear iron centers. Since the only difference between tyrosine and phenylalanine is the lack of the hydroxyl group, the absence of this hydrogen bond in the Y122F mutant protein could result in the more negative midpoint potential observed with the mutant protein. In fact the difference in the midpoint potentials (ΔE = 63 mV) is commensurate with the loss of a weak hydrogen bond (2.4−12 kcal) (Frey et al., 1994). The absence of this hydrogen bond may also be responsible for the slow kinetics observed during the reduction of the Y122F mutant protein. If the formation of the hydrogen bond between Y122 and D84 upon reduction is necessary for stabilization of the reduced form of the protein, the absence of this bond could make formation of the reduced structure difficult.

Our redox data suggests that the hydrogen bond between Y122 and D84 is present in all the reduced forms of the protein studied. As shown in Table 4, in three of the four different types of experiments that we have conducted, the potential difference between the wild type and mutant R2 proteins remains approximately 60 mV. The difference between the wild type and Y122F R2 proteins is 63 mV in water, 45 mV in the presence of azide, and 65 mV upon binding of R1. Only in the D_2O experiments do we see the potentials of the wild type and Y122F R2 proteins approach the same value. In this case, deuterium exchange appears to perturb the protein structure significantly. Thus, the accumulated data strongly indicates that the hydrogen bond in the reduced protein is present in all experiments with the wild type protein and absent in the mutant protein. The absence of this hydrogen bond in the Y122F protein destabilizes the diiron(II) state relative to the diiron(III) state, engendering the observed cathodic shifts.

The observed negative shift in the redox potential for the diiron center upon the addition of azide suggests that the azide is indeed binding to the dinuclear iron center. Even the addition of a very low molar ratio of azide to iron results in a negative shift in the midpoint potential. This negative trend continues until a molar ratio of almost two azide per four irons is obtained, where the potential levels off and does not decrease further until a large excess of azide is added. These results support the binding of one azide molecule per iron center. Whether a second molecule of azide binds to

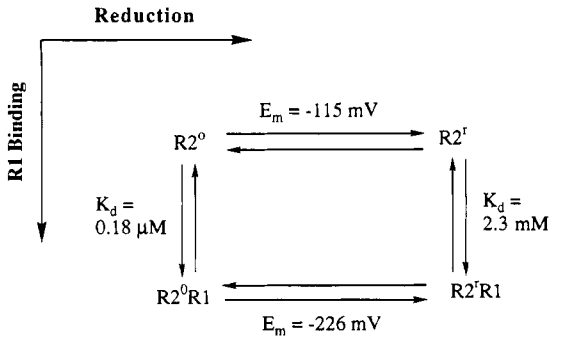

FIGURE 10: Thermodynamic energy coupling of the R2 reduction and R1 binding process. The diiron (III) form of $R2_{met}$ ($R2^o$) can be reduced to the diiron (II) state ($R2^r$). Both of these states can bind R1, but the R1 dependent shift in the midpoint potential values requires that the affinity of the R1−R2 complex be dependent upon the redox state of the dinuclear iron centers.

the diiron(II) center cannot be determined, since the midpoint potential of the centers only decreases in the presence of a large excess of azide and then the decrease is only −11 mV. The negative shift in the redox potential points to a preferential binding to the diiron(III) centers at substoichiometric amounts of azide. The ratio of the binding constants for azide binding to the oxidized and reduced forms of the diiron center can be calculated from eq 3. Using the midpoint potential when one azide per diiron center is believed to be bound (−207 mV), the ratio of K_{d2}/K_{d1} = 2555. This value shows that the dissociation constant for azide binding to the diiron(II) center is much larger than that of the diiron(III) center. This is further supported by the midpoint potentials determined during the reversibility experiment which exhibits a large amount of hysteresis. In the reductive direction, when azide is bound, the potential is more negative (−186 mV). In the oxidative direction, where azide is most likely unbound, the potential is more positive (−127 mV) and approaches that of the diiron center when no azide is present (−115 mV).

The binding of R1 to R2 also causes a large negative shift in the midpoint potential which probably results from a conformational change that stabilizes the oxidized form of the R2 protein. The lack of iron spectral changes in the visible spectrum suggests that this conformational change is subtle and may involve alterations in the intricate hydrogen bonding network associated with the diiron cluster (Nordlund & Eklund, 1993; Åberg et al., 1993). This negative shift in midpoint potential also indicates that the dissociation constant for the R1−R2 complex (calculated via eq 3) has increased by at least 3−4 orders of magnitude for the $R1-R2_{red}$ complex (Figure 10). The increased dissociation constant supports the notion that the oxidized form of the R2 protein is preferably bound over the reduced, favoring the catalytically active form of the protein for substrate turnover. Therefore, the tyrosyl radical is present upon binding and the reduction of ribonucleotides can begin instantaneously upon complex formation.

The large increase in the dissociation constant for the $R1-R2_{red}$ complex means that the $R1-R2_{red}$ complex is not saturated under these experimental conditions. Experiments in which saturating conditions would prevail were not possible for several reasons. First, such experiments would require gram quantities of R1. Equilibration is not possible at such high concentrations with our methodology. Second, the equilibration time frame (6 h per point, 36 h per experiment) is at the limit of protein stability. Finally, any attempts to increase the indicator dye concentration to speed equilibrium resulted in the complete loss of the R2 spectrum and inaccurate dye subtractions. Therefore, while some shift in the absolute $R1-R2_{red}$ midpoint potential and dissociation constant could be expected under saturating conditions, a shift in the relative magnitude of these values would not be observed.

Finally, the binding of R1 could also play a regulatory role in the redox cycling of the R2 protein. Previous work in our laboratory has set the precedent for such component regulation. Such thermodynamic regulation has been observed in both the medium chain acyl CoA dehydrogenase (MCAD) system and MMOH. For MCAD, our work determined that the binding of product shifts the redox potential of the flavin positive by over 100 mV (Lenn et al., 1990; Lenn, 1989; Johnson et al., 1995), providing the thermodynamic driving force for electron transfer to the enzyme. In the case of MMOH, the binding of component B (MMOB) results in a negative redox potential shift of −132 mV (Paulsen et al., 1994) for the dinuclear iron center, thermodynamically prohibiting the transfer of electrons to the protein in the redox cycle. The binding of the reductase component (MMOR) then shifts the redox potential of the protein back to its original value (Paulsen et al., 1994), allowing for electron transfer when the entire multicomponent system is formed.

In the case of R2, there is a NAD(P)H:flavin oxidoreductase or NAD(P)H flavinsulfite reductase that is involved in the reduction of the dinuclear iron centers (Fontecave et al., 1987; Coves et al., 1993). The function of both reductases is to catalyze the reduction of either free or protein-bound flavins (riboflavin, flavin mononucleotide, and flavin adenine dinucleotide) which then reduce the diiron center. For the sulfite reductase, riboflavin was found to be the best substrate of the free flavins (Coves et al., 1993) and has a redox potential of −174 mV under our experimental conditions. The redox potentials of the oxidoreductase is not known, but typical oxidoreductases generally have potentials in the −200 mV range, as found for MMOR from *Methylococcus capsulatus* (E_m = −205 mV) (Lund & Dalton, 1985) and CDP-6-deoxy-Δ-3,4-glucoseen reductase expressed from *E. coli* (E_m = −210 mV).[2] Thus, the binding of R1 to R2 causes a negative shift in the R2 potential which would thermodynamically prohibit the reduction of the dinuclear iron centers by a flavin or flavoprotein. This ensures that external reductants in the cell medium will not inactivate the active R1−R2 complex during turnover and requires that redox cycling of the R2 protein occur when it is not bound to R1. Reduction of the diiron(III) center could cause the electrons to be transferred to the tyrosyl radical, generating an inactive form of the protein. If the dinuclear iron center is reduced (E_m = −115 mV) in the absence of oxygen, there would be a tremendous thermodynamic driving force for the reduction of the tyrosyl radical ($E^{\circ\prime}$ = +1000 mV). It is not clear from our work if the reduced diiron center is kinetically capable of transferring electrons to the radical, since we cannot absolutely determine if the electrochemical reductant methyl viologen is interacting with both redox centers or if only the dinuclear iron center is accepting the electrons and then shuttling them to the tyrosyl radical, as would be predicted by thermodynamics. This regulation

[4] M. Fontecave, personal communication.

would furthermore prevent energy waste in the cell due to unnecessary cycling of the R2 protein when no substrate is present. This proposed regulatory pathway is supported by the observation that the R1−R2 complex can not be reduced by the reductase−flavin system.[4] The fact that the same degree of negative shift is experienced when R1 is bound to the Y122F protein demonstrates that this shift is consistent for the dinuclear iron centers and is not dependent upon the presence of the Y122 residue.

In conclusion, the complete thermodynamic properties of the R2 protein from *E. coli* have been reported. The catalytically essential Y122 radical has a redox potential of 1000 ± 100 mV, while the diiron centers have a potential of −115 mV, consistent with the presence of an oxo bridge and a carboxylate-rich ligand environment. The diiron centers are reduced by a two-electron process, making R2 unique among other nonheme dinuclear iron proteins in not having a readily accessible mixed valence form. We speculate that this $2e^-$ process is an important feature of its dioxygen activation mechanism. The investigation of the Y122F R2 mutant protein has provided the first solid evidence that this essential residue significantly influences the dinuclear iron center by modulating its redox properties. Finally, R1 binding results in a large negative shift in the midpoint potential of the diiron center. This striking result demonstrates that the R1 protein preferentially binds to the oxidized form of R2 and provides for thermodynamic regulation of the redox cycling of the latter protein.

ACKNOWLEDGMENT

We acknowledge Prof. JoAnne Stubbe and Dr. Martin Bollinger, Jr., (Massachusetts Institute of Technology) for providing the data for the tyrosyl radical quantitation.

REFERENCES

Åberg, A. (1993) Ph.D. Thesis, University of Stockholm, Stockholm, Sweden.
Åberg, A., Nordlund, P., & Eklund, H. (1993) *Nature 361I*, 276−278.
Armstrong, F. A., Harrington, P. C., & Wilkins, R. G. (1983) *J. Inorg. Biochem. 18*, 83−91.
Atkin, C. L., Thelander, L., & Reichard, P. (1973) *J. Biol. Chem. 21*, 7464−7472.
Bollinger, J. M., Jr., Edmondson, D. E., Huynh, B. H., Filley, J., Norton, J. R., & Stubbe, J. (1991) *Science 253*, 292−298.
Bollinger, J. M., Jr., Tong, W. H., Ravi, N., Huynh, B. H., Edmondson, D. E., & Stubbe, J. (1994a) *J. Am. Chem. Soc. 116*, 8015−8023.
Bollinger, J. M., Jr., Tong, W. H., Ravi, N., Huynh, B. H., Edmondson, D. E., & Stubbe, J. (1994b) *J. Am. Chem. Soc. 116*, 8024−8032.
Clark, W. M. (1960) in *Oxidation−Reduction Potentials of Organic Systems*, Williams and Wilkins, New York.
Climent, I., Sjöberg, B.-M., & Huang, C. Y. (1992) *Biochemistry 31*, 4801−4807.
Còves, J., Nivière, V., Eschenbrenner, M., & Fontecave, M. (1993) *J. Biol. Chem. 268*, 18604−18609.
Davydov, R., Kuprin, S., Gräslund, A., & Ehrenberg, A. (1994) *J. Am. Chem. Soc. 116*, 11120−11128.
DeFelippis, M. R., Murthy, C. P., Faraggi, M., & Klapper, M. H. (1989) *Biochemistry 28*, 4847−4853.
DeRose, V. J., Liu, K. E., Kurtz, D. M., Hoffman, B. M., & Lippard, S. J. (1993) *J. Am. Chem. Soc. 115*, 6440−6441.
Duggleby, R. G. (1981) *Anal. Biochem. 110*, 9−18.
Einarsdottir, G. H., Stankovich, M. T., & Tu, S. C. (1988) *Biochemistry 27*, 3277−3285.
Elgren, T. E., Lynch, J. B., Juarez-Garcia, C., Münck, E., Sjöberg, B.-M., & Que, L., Jr. (1991) *J. Biol. Chem. 266*, 19265−19268.
Elgren, T. E., Hendrich, M. P., & Que, L., Jr. (1993) *J. Am. Chem. Soc. 115*, 9291−9292.
Fontecave, M., Eliasson, R., & Reichard, P. (1987) *J. Biol. Chem. 262*, 12325−12331.
Frey, P. A., Whitt, S. A., & Tobin, J. B. (1994) *Science 264*, 1927−1930.
Gerez, C., Gaillard, J., Latour, J. M., & Fontecave, M. (1991) *Angew. Chem., Int. Ed. Engl. 30*, 1135−1136.
Hendrich, M. P., Münck, E., Fox, B. G., & Lipscomb, J. D. (1990) *J. Am. Chem. Soc. 112*, 5861−5865.
Hendrich, M. P., Elgren, T. E., & Que, L., Jr. (1991) *Biochem. Biophys. Res. Comm. 176*, 705−710.
Johnson, B. D., Macini-Samuleson, G., & Stankovich, M. T. (1995) *Biochemistry 34*, 7047−7055.
Lam, K.-Y., Fortier, D. G., & Sykes, A. G. (1990) *J. Chem. Soc., Chem. Commun.* 1019−1021.
Lenn, N. D. (1989) M.S. Thesis, University of Minnesota, Minneapolis, MN.
Lenn, N. D., Stankovich, M. T., & Liu, H. (1990) *Biochemistry 29*, 3709−3715.
Lund, J., & Dalton, H. (1985) *Eur. J. Biochem. 147*, 291−296.
Lynch, J. B. (1989) Ph.D. Thesis, University of Minnesota, Minneapolis, MN.
Lynch, J. B., Juarez-Garcia, C., Münck, E., & Que, L., Jr. (1989) *J. Biol. Chem. 264*, 8091−8096.
Mao, S. S., Holler, T. P., Bollinger, J. M., Jr., Yu, G. X., Johnston, M. I., & Stubbe, J. (1992a) *Biochemistry 31*, 9744−9751.
Mao, S. S., Yu, G. X., Chalfoun, D., & Stubbe, J. (1992b) *Biochemistry 31*, 9752−9759.
Nordlund, P. (1990) Ph.D. Thesis, Swedish University of Agricultural Sciences, Uppsala, Sweden.
Nordlund, P., & Eklund, H. (1993) *J. Mol. Biol. 232*, 123−164.
Nordlund, P., Sjöberg, B.-M., & Eklund, H. (1990) *Nature 345*, 593−598.
O'Reilly, J. E. (1973) *Biochim. Biophys. Acta 292*, 509−515.
Ormö, M., Regnström, K., Wang, Z., Que, L., Jr., Sahlin, M., & Sjöberg, B.-M. (1995) *J. Biol. Chem. 270*, 6570−6576.
Paulsen, K. E., Liu, Y., Fox, B. G., Lipscomb, J. D., Münck, E., & Stankovich, M. T. (1994) *Biochemistry 33*, 713−722.
Petersson, L., Gräslund, A., Ehrenberg, A., Sjöberg, B.-M., & Reichard, P. (1980) *J. Biol. Chem. 255*, 6706−6712.
Que, L., Jr., & True, A. E. (1990) *Prog. Inorg. Chem. 38*, 97−201.
Ravi, N., Bollinger, J. M., Jr., Huynh, B. H., Edmondson, D. E., & Stubbe, J. (1994) *J. Am. Chem. Soc. 116*, 8007−8014.
Reem, R. C., & Solomon, E. I. (1987) *J. Am. Chem. Soc. 109*, 1216−1226.
Rosenzweig, A. C., Frederick, C. A., Lippard, S. J., & Nordlund, P. (1993) *Nature 366*, 537−543.
Sahlin, M., Petersson, L., Gräslund, A., Ehrenberg, A., Sjöberg, B.-M., & Thelander, L. (1987) *Biochemistry 26*, 5541−5548.
Sahlin, M., Gräslund, A., Petersson, L., Ehrenberg, A., & Sjöberg, B.-M. (1989) *Biochemistry 28*, 2618−2625.
Sjöberg, B. M., Loehr, T. M., & Sanders-Loehr, J. (1982) *Biochemistry 21*, 96−102.
Stankovich, M. T. (1980) *Anal. Biochem. 109*, 295−308.
Stankovich, M. T., & Fox, B. G. (1983) *Biochemistry 22*, 4466−4472.
Stubbe, J. (1990) *J. Biol. Chem. 265*, 5329−5332.
Thelander, L., & Reichard, P. (1979) *Annu. Rev. Biochem. 48*, 133−158.
Thomann, H., Bernardo, M., McCormick, J. M., Pulver, S., Andersson, K. K., Lipscomb, J. D., & Solomon, E. I. (1993) *J. Am. Chem. Soc. 115*, 8881−8882.
Walsh, C. (1979) in *Enzymatic Reaction Mechanisms* (Bartlett, A. C., & McCombs, L. W., Eds.) pp 108−131, W. H. Freeman, New York.
Wang, D. L., Holz, R. C., David, S. S., Que, L., Jr., & Stankovich, M. T. (1991) *Biochemistry 30*, 8187−8194.
Wilkinson, G., Rosenblum, M., Whiting, M. C., & Woodward, R. B. (1952) *J. Am. Chem. Soc. 74*, 2125−2126.

BI951039X